Review | Vol. 29, No. 16 / 2 August 2021 / Optics Express 24816

Optics EXPRESS

Smart thermal management with near-field thermal radiation [invited]

IVAN LATELLA,[1] SVEND-AGE BIEHS,[2] AND PHILIPPE BEN-ABDALLAH[3,*]

[1]Departament de Física de la Matèria Condensada, Universitat de Barcelona, Martí i Franquès 1, 08028 Barcelona, Spain
[2]Institut für Physik, Carl von Ossietzky Universität, D- 26111 Oldenburg, Germany
[3]Laboratoire Charles Fabry, UMR 8501, Institut d'Optique, CNRS, Université Paris-Saclay, 2 Avenue Augustin Fresnel, 91127 Palaiseau Cedex, France
*pba@institutoptique.fr

Abstract: When two objects at different temperatures are separated by a vacuum gap they can exchange heat by radiation only. At large separation distances (far-field regime), the amount of transferred heat flux is limited by Stefan-Boltzmann's law (blackbody limit). In contrast, at subwavelength distances (near-field regime), this limit can be exceeded by orders of magnitude thanks to the contributions of evanescent waves. This article reviews the recent progress on the passive and active control of near-field radiative heat exchange in two- and many-body systems.

© 2021 Optical Society of America under the terms of the OSA Open Access Publishing Agreement

1. Introduction

The control of electron flow in solids is at the origin of modern electronics which has revolutionized our daily life. The diode and the transistor introduced by Braun [1] and Bardeen [2], respectively are undoubtedly the cornerstones of modern information technologies. Such devices allow for rectifying, switching, modulating and even amplifying the electric currents. Astonishingly, until very recently no thermal analogs of these building blocks were devised to exert a similar control on the heat flux. An important step forward in this direction has nevertheless been carried out by Baowen Li and co-workers [3,4] and by Chang et al. [5] at the beginning of 2000's, when they proposed a phononic counterpart of the diode and transistor [6]. These pioneer works have paved the way to a technology, also called "thermotronics" in analogy to traditional electronics, where electrical currents and voltage biases are replaced by heat currents and temperature biases to control heat conduction though a network of solid elements. A recent review [7] summarizes the last developments carried out to control heat flux carried by conduction at both macroscale and microscale using artificial structures.

However, heat transport mediated by phonons in solid networks suffers from some weaknesses of fundamental nature which intrinsically limit the performance of this technology. One of these limitations is linked to the speed of acoustic phonons itself (the speed of sound) which bounds the operational speed of these devices. Another intrinsic limitation of phononic devices is the presence of local Kapitza resistances which come from the mismatch of vibrational modes supported by the different solid elements in the network. This resistance can drastically reduce the heat transported across the system. To overcome these limitations, concepts for a purely photonic technology have been proposed as an alternative way to handle heat transfer at the nanoscale. In the present work, we review recent developments carried out in this direction. After briefly introducing the theoretical framework commonly used to described the radiative heat transfer in the near-field regime between two or several solid bodies, we describe the main physical mechanisms and related device concepts which allow for a passive and active control of radiative heat transfer at the nanoscale. Finally, we conclude this review by suggesting future research directions for advanced thermal management with thermal photons.

#433539 https://doi.org/10.1364/OE.433539
Journal © 2021 Received 11 Jun 2021; revised 6 Jul 2021; accepted 7 Jul 2021; published 20 Jul 2021

Optics EXPRESS

2. Some basics on the near-field heat transfer

The radiative heat transfer between distant objects, in the far field, is bounded by the blackbody limit given by the Stefan-Boltzmann law [8]. The transport of heat in this situation is mediated by propagating modes of the electromagnetic radiation emitted by the objects. When separation distances are smaller than the thermal wavelength λ_T defined by Wien's displacement law, which is about 10 μm at room temperature, near-field effects become relevant due to the contribution of evanescent modes of the electromagnetic field confined close to the surface of the objects. By bringing them at separations $d<\lambda_T$, the blackbody limit can notably be overcome owing to this near-field contribution from evanescent waves [9–13]. Hence, the radiative heat flux exchanged in near-field between two silica samples separated by a distance $d = 100\,nm$ around the ambient temperature with a temperature gradient $\Delta T = 50\,K$ is $\phi \simeq 20000\,W.m^{-2}$, while the blackbody limit is $\phi_{BB} = \sigma T^3 \Delta T \simeq 75\,W.m^{-2}$ and the solar flux used for conventional photovoltaics is about $\phi_S = 1000\,W.m^{-2}$, σ being the Stefan-Boltzmann constant.

The near-field radiative heat exchange in a given configuration of several solid objects in a thermal non-equilibrium situation are commonly calculated in the framework of fluctuational electrodynamics. To illustrate the basic principles of this approach, let us consider the simple example of two objects with volumes V_1 and V_2 held at temperatures T_1 and T_2 which are separated by a vacuum gap of thickness d as sketched in Fig. 1. The thermal motion of charges within each of these objects induce fluctuational current densities $\mathbf{j}_i(\mathbf{r},\omega)$ $(i = 1,2)$ which themselves induce fluctational electric and magnetic fields $\mathbf{E}_i$ and $\mathbf{H}_i$ fulfilling the stochastic Maxwell equations [14]

$$\nabla \times \mathbf{E}_i(\mathbf{r},\omega) = \quad i\omega\mu_0 \mathbf{H}_i(\mathbf{r},\omega), \tag{1}$$

$$\nabla \times \mathbf{H}_i(\mathbf{r},\omega) = \quad -i\omega\epsilon_0\epsilon_i(\mathbf{r},\omega)\mathbf{E}_i(\mathbf{r},\omega) + \mathbf{j}_i(\mathbf{r},\omega), \tag{2}$$

where $\epsilon_i(\mathbf{r},\omega)$ denotes the local dielectric tensor of object i (here assumed to be non-magnetic) at point $\mathbf{r}$; ϵ_0 and μ_0 are the permittivity and permeability of vacuum. The linearity of these equations allows us to relate $\mathbf{E}_i$ and $\mathbf{H}_i$ to the source currents $\mathbf{j}_i(\mathbf{r},\omega)$ as follows [14]

$$\mathbf{E}_i(\mathbf{r},\omega) = i\omega\mu_0 \int_{V_i} \mathrm{d}^3 r'\, \mathbb{G}^{EE}(\mathbf{r},\mathbf{r'})\mathbf{j}_i(\mathbf{r'},\omega), \tag{3}$$

$$\mathbf{H}_i(\mathbf{r},\omega) = i\omega\mu_0 \int_{V_i} \mathrm{d}^3 r'\, \mathbb{G}^{HE}(\mathbf{r},\mathbf{r'})\mathbf{j}_i(\mathbf{r'},\omega), \tag{4}$$

where $\mathbb{G}^{EE}$ and $\mathbb{G}^{HE}$ denote the linear electric and magnetic response tensors also called the dyadic Green functions of the system. From these expressions one can determine the mean Poynting vector

$$\langle \mathbf{\Pi}_i(\mathbf{r},\omega)\rangle = 2\mathcal{R}e\langle \mathbf{E}_i \times \mathbf{H}_i^*\rangle \tag{5}$$

which can be readily expressed in terms of both the Green tensor components and the correlations functions of fluctuating currents. Assuming that the objects are in local thermal equilibrium, then according to the fluctuation-dissipation theorem these correlations are related to the local temperature by the following expression [15]

$$\langle j_{i,\mu}(\mathbf{r},\omega) j^*_{i,\nu}(\mathbf{r}',\omega)\rangle = \frac{2\hbar\omega^2\epsilon_0}{\pi}[\epsilon_{i,\mu\nu}(\mathbf{r},\omega) - \epsilon^*_{i,\nu\mu}(\mathbf{r},\omega)]n(\omega,T_i)\delta(\mathbf{r}-\mathbf{r}'), \tag{6}$$

where $\hbar$ is the Planck constant and $n(\omega,T_i) = 1/(\exp[\hbar\omega/k_\mathrm{B}T_i] - 1)$ is the Bose-Einstein distribution function at temperature T_i; k_B is the Boltzmann constant. It follows that the Poynting vector can be expressed in terms of all local temperatures inside the system. The spectral radiative

Optics EXPRESS

power $P_{1\leftrightarrow 2}(\omega)$ exchanged between the two objects can be obtained by integrating the flux expressed by the Poynting vector over the surfaces $A_i = \partial V_i$ of two bodies as follows

$$P_{1\leftrightarrow 2}(\omega) = \int_{A_2} \mathbf{dA_2} \cdot \langle \mathbf{\Pi}_1(\mathbf{r}, \omega)\rangle - \int_{A_1} \mathbf{dA_1} \cdot \langle \mathbf{\Pi}_2(\mathbf{r}, \omega)\rangle. \tag{7}$$

Note, that here this expression is only valid as long as the source currents in both objects are uncorrelated [14]. Finally, the net power exchanged between the two bodies is obtained by summation over all frequencies (i.e. $\mathcal{P}_{net} = \int_0^\infty \frac{d\omega}{2\pi} P_{1\leftrightarrow 2}(\omega)$). In many-body systems this approach can be generalized to take into account all multiscattering processes [16–20]. Formally the net power received by each object can be written in a Landauer-like form as

$$\mathcal{P}_i = \sum_{k\neq i} \int_0^\infty \frac{d\omega}{2\pi} \hbar\omega [n(\omega, T_k)\mathcal{T}_{ki}(\omega) - n(\omega, T_i)\mathcal{T}_{ik}(\omega)], \tag{8}$$

where the transmission functions $\mathcal{T}_{ik}$ are related to the coupling efficiency of modes at the frequency ω between the body i and body k. Explicit expressions for many-particle systems within the dipole model and for multilayer systems can be found in Ref. [16] and Ref. [17], respectively, and general expressions derived within the scattering-matrix approach can be found in Ref. [18]. For more details on the many-body theory and an extensive list of works on this topic we refer to the review [20]. Generally the transmission functions depend on the geometric configuration and in particular on the distance between the objects i and k as well as on the optical material properties $\epsilon_{i,\mu\nu}$ and $\epsilon_{k,\mu\nu}$. This opens up the possibility to tune the heat transfer by changing the configuration of the involved objects. More interesting, if the material properties significantly depend on temperature, external electric or magnetic fields, the heat flux can be actively controlled by changing these quantities.

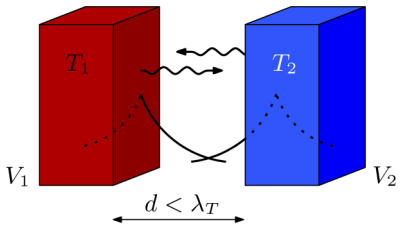

Fig. 1. Sketch of radiative heat exchanges between two solids of volumes V_1 and V_2 held at temperatures T_1 and T_2 and separated by a vacuum gap of thickness d. At large separation distances, heat exchanges are mediated by propagating photons (wavy arrows). At subwavelength distances ($d<\lambda_T$, λ_T being the thermal wavelength), the heat transfer is enhanced by the the contribution of evanescent waves localized on the surface of bodies.

3. Rectification

The diode is one of the fundamental building blocks to control electron currents in electronic systems. In an electronic diode (Fig. 2(a)), the current can flow mainly in one direction when a bias voltage is applied through its two terminals. This corresponds to a strong asymmetry due to a nonlinearity in the electrical conductance. As in the case of electronics, one of the basic devices to impose directionality of radiative heat flows are the thermal diodes. When a temperature bias $T_1 - T_2$ is applied between two separated solids with temperatures T_1 and T_2, the magnitude of the heat flux they exchange by radiation generally does not depend on the sign of this bias. However, in presence of temperature-dependent material properties of the receiver or emitter, an asymmetry can appear between the heat flux P^f in the forward biased situation ($T_1 - T_2>0$) and

Optics EXPRESS

the heat flux P^r in the reverse scenario ($T_1 - T_2 < 0$), such that $P^f \neq P^r$. Hence, radiative thermal rectification can be achieved under these conditions. Notice that here P^f and P^r are assumed positive, since they represent the heat flowing from the hottest to the coldest terminal in the two temperature biased scenarios.

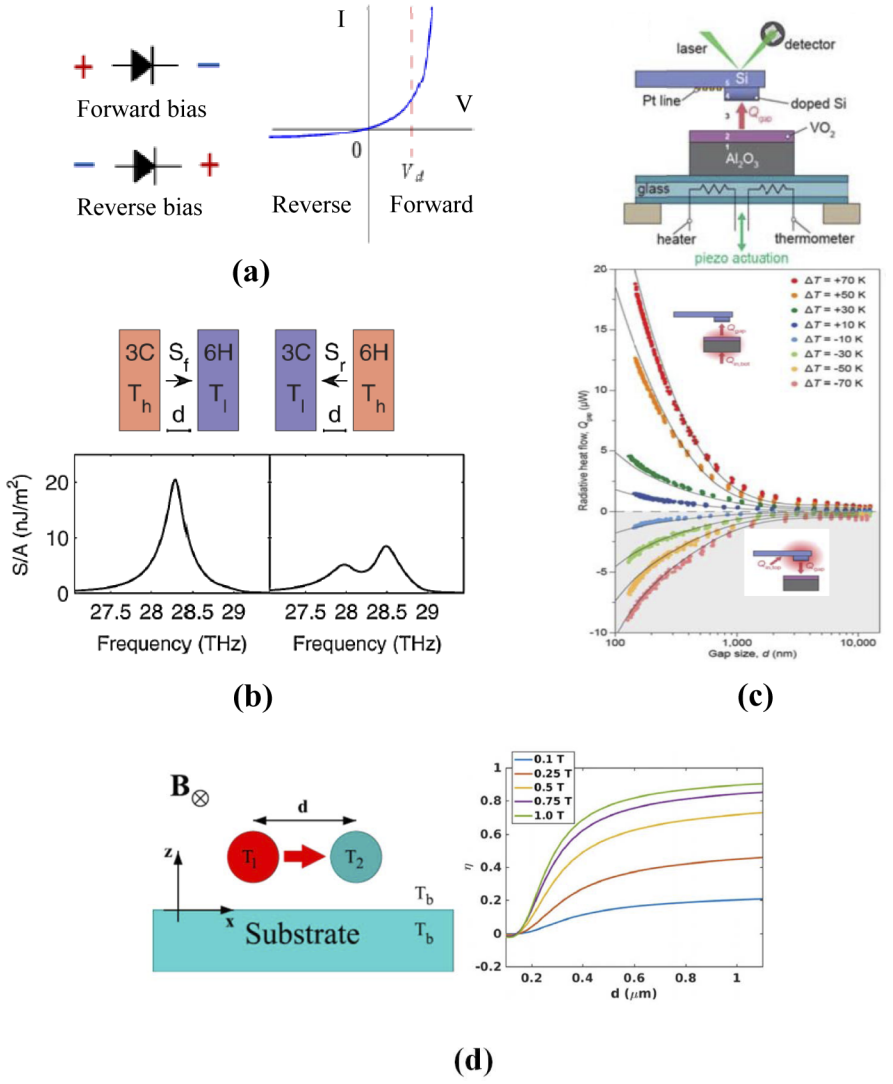

Fig. 2. (a) Sketch of an electric diode and its typical current-voltage curve. (b) Schematic of a near-field thermal rectifier made with a slab of 3*C*-SiC and a slab of 6*H*-SiC in the forward (f), and the reverse (r) scenarios and the corresponding spectra of net heat flux. Reproduced with permission from [21]. (c) Schematic of a microfabricated VO_2 based (phase-change material) radiative diode and measured near-field heat flux vs. the temperature bias ΔT in the forward ($\Delta T > 0$) and the reverse ($\Delta T < 0$) scenarios. Reproduced with permission from [39]. (d) Radiative thermal diode driven by nonreciprocal surface waves: the surface waves induce an asymmetry in the heat transfer between two magneto-optical nanoparticles placed close to a magneto-optical substrate in presence of a magnetic field B. This asymmetry is quantified by the rectification coefficient $\eta = (P_1 - P_2)/P_1$, where P_1 is the power received by particle 1 when $T_2 > T_1$ (backward scenario) while P_2 is the power received by particle 2 in the opposite situation (forward scenario). Reproduced with permission from [47].

Optics EXPRESS

As happens with the electronic counterparts, radiative thermal diodes act as a good radiative thermal conductor for a given sign of the temperature bias, while they behave as an insulator in the opposite situation. A first thermal radiative rectifier (Fig. 2(b)) has been introduced by Otey et al. in 2010 [21] using two different polytypes of SiC having different temperature-dependent optical properties. In this case, the transmission function $\mathcal{T}_{12}$ depends implicitly on the temperature of the two solids through the temperature dependence of their reflection coefficients r_1 and r_2. Thus, in the forward scenario with a low temperature T and a high temperature $T + \Delta T$ we formally have a transmission function of the form

$$\mathcal{T}_{12}^{f} = \mathcal{T}_{12}(r_1(T + \Delta T), r_2(T)), \tag{9}$$

while in the reverse scenario this function reads

$$\mathcal{T}_{12}^{r} = \mathcal{T}_{12}(r_1(T), r_2(T + \Delta T)). \tag{10}$$

The heat transport asymmetry in the device can then be evaluated with the (normalized) rectification coefficient

$$R = \frac{|P^f - P^r|}{\max(P^f, P^r)}. \tag{11}$$

When the interacting solids have weakly temperature dependent optical properties, R is relatively small provided that the temperature bias is small as well. Hence, a rectification coefficient of up to $\approx 29\%$ has been reported [21] in near-field regime between two planar slabs of $3C$-SiC and $6H$-SiC with $\Delta T = 300$ K or between slabs covered by an optimized coating [22] or slabs made with doped semiconductors with different doping levels and different thicknesses [23]. On the other hand, rectification coefficients as high as 90% have been reported between two solids when the temperature bias becomes large [24–26].

In 2013, phase-change materials have been proposed [27–29] to improve the asymmetry of the radiative transport in configurations leading to large rectification coefficients with a relatively small temperature bias. These materials undergo a sudden and drastic change in their optical properties around their critical temperature. Among these materials, metal-insulator transition (MIT) materials have attracted significant attention to design radiative heat rectifiers [27–34]. A widely MIT material is vanadium dioxide (VO_2) which undergoes its phase transition at $T_c \approx 340$ K [35,36]. Thanks to this transition rectification coefficients higher than 70% have been predicted and highlighted in far-field regime [27,37,38] with a temperature bias ΔT<50 K and values around 90% have been observed in near-field regime [29,39–41]. Furthermore, materials undergoing a normal-metal-superconductor transition [42–46] have also been considered to design radiative thermal rectifiers operating at cryogenic temperatures with similarly good performances.

Non-reciprocal materials have also been considered to break the symmetry in the heat transport berween two bodies. Rectification factors close to 90% have been recently predicted [47] in systems made with magneto-optical (MO) particles placed above a MO substrate (Fig. 2(d)) and exchanging heat via surface waves.

Finally, a concept of many-body rectifier working by embedding a passive intermediate body interacting with the two terminals, has been recently introduced [48]. Unlike the classical thermal rectification discussed above which require a noticeable temperature dependence of the optical properties of the materials, here the asymmetry in the heat transport results only from many-body interactions. Hence they can rectify the heat flux over a broad temperature range.

4. Modulation and switching

Controlling the magnitude and the direction of heat flux exchanged between solids at nanoscale is of prime importance in many technological applications and considerable effort has been made

Optics EXPRESS

these last years to develop new strategies to this end. Below we discuss the recent developments carried out in this direction.

The most natural way to control the magnitude of flux exchanged between two solids is by changing their separation distance d. In near-field regime the transmission coefficient scales like $\mathcal{T}_{12} \propto 1/d^n$, where $n = 6$ for two nanoparticles, $n = 3$ for a spherical object in vicinity of a slab, and $n = 2$ for two slabs, for instance. It follows that a displacement of one decade from a given position modifies the heat flux by orders of magnitude. This property can be exploited by mechanically changing the separation distance between two objects to modulate or switch the near-field radiative heat flux. Furthermore, micro/nano electromechanical systems (MEMS/NEMS) have been developped [49–51] in the last years which allow for performing a high precision control of the separation distance between two solids in the subwavelength regime, up to distances of few tens of nanometers, by tuning the electrostatic interaction between the solids using an actuation potential (Fig. 3(a)). MEMS technology can be used for an active thermal management at nanoscale or to harvest on demand the near-field energy confined at the surface of hot objects using tunable near-field thermophotovoltaic converters [50]. Besides this control of near-field heat exchanges through a change of the separation distance between the solids, multiscattering effects induced by the presence of a third body has been proposed [52] to tune the heat exchanges in the near-field between two solids (Fig. 3(b)). By bringing a third body (even non-emitting) close to the emitter and receiver the heat flux exchanged between these bodies can be either amplified or inhibited thanks to many-body interactions.

Another way to control mechanically the near-field heat exchanges between two solids is the change of their relative orientation keeping their separation distance constant. This can have a strong impact in the coupling effciency of evanescent modes supported by each solid and therefore on the heat flux they exchange. Such change can simply be achieved using textured solids in relative rotation. For instance, the radiative heat flux between two uniaxial slabs with optical axis within the interface can be tuned by relative rotation of one slab [53] as shown for two grating structures in Fig. 3(c). When the optical axes are aligned, the heat flux is maximal and when the optical axis are perpendicular to each other the heat flux has a minimum. This effect can of course be exploited for any two anisotropic media, and it has already been demonstrated [54] for two natural hyperbolic materials like hexagonal Boron Nitride (hBN). It must be noted that the operating speed of these mechanical control is intrinsically limited by the thermalization time of its components. With nanostructures interacting in near-field this time is typically in the order of few milliseconds. Moreover, it is worth to point out that mechanical controlled actuation may be difficult to implement in certain situations and moving parts in any device are usually not desirable because of wear and tear. Beside the mechanical control of the separation distance and relative orientation strain-controled switches have been recently proposed to tune the flux. In these systems an intermediate layer of material, whose permittivity is controlled with mechanical strain, drives the radiative heat flux between a source and a drain at fixed separation distances [55].

As shown in the previous section MO materials can also be used to control actively the near-field heat exchanges between two solids using an external magnetic field. This possibility has been first suggested by Moncada-Villa et al. [56,57] who have shown that a change of the magnitude of magnetic field can significantly modify both the nature and the coupling of evenescent modes. More recently new thermomagnetic effects in MO systems [19,58] have opened the way to a new strategy for controlling near-field heat exchanges. The first effect is a giant magneto-resistance [19] which enables a significant increase of the thermal resistance along MO nanoparticle networks (Fig. 3(d)) with increasing magnitude of an external magnetic field. This giant resistance results from a strong spectral shift of localized surface waves supported by the particles under the action of a magnetic field. Recent works have combined MO materials and dielectrics in a hyperbolic multilayer structure [58,59], because on the one hand the formation

Optics EXPRESS

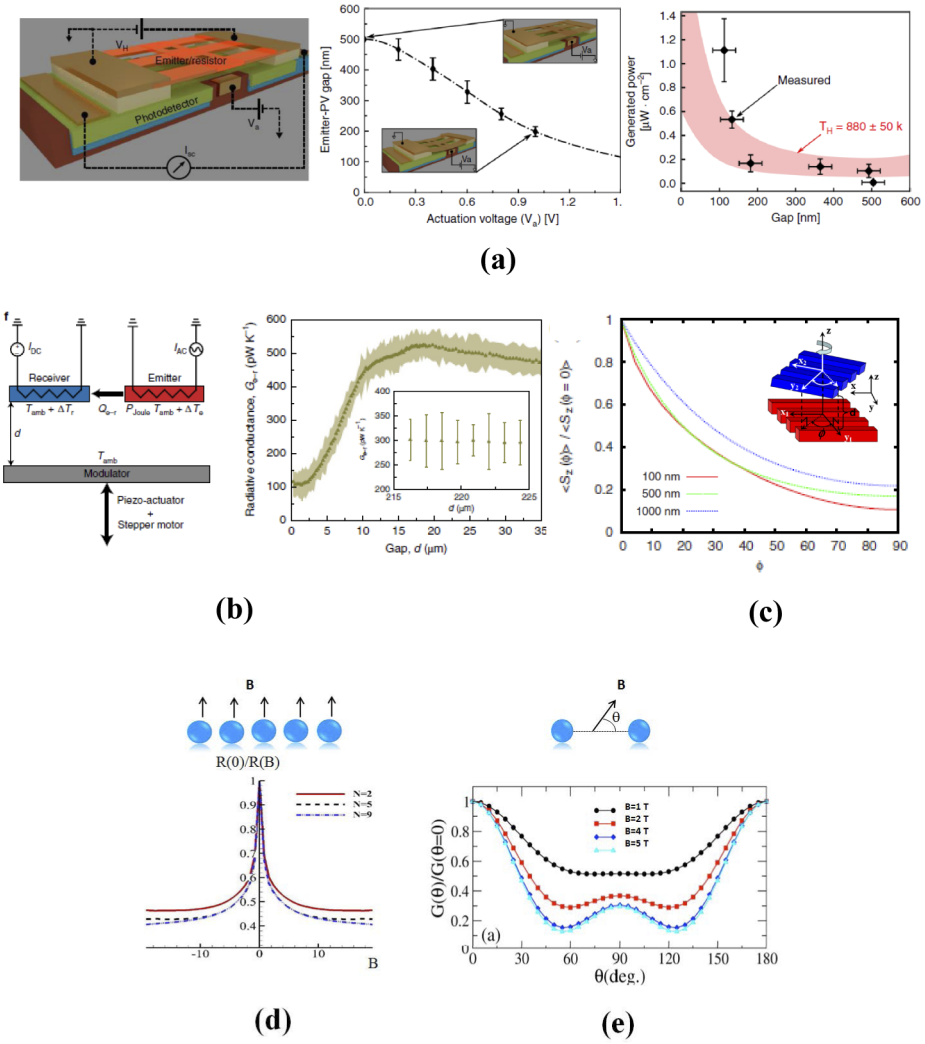

Fig. 3. (a) Nano-electromechanical thermal switch. The NEMS consists in a suspended bridge (thermal emitter) which is brought closer to a solid through application of an actuation potential V_a. Their separation distance and the heat flux they exchange can be controlled with V_a. Reproduced with permission from [50]. (b) Active control of heat flux exchanged between two solids. The thermal conductance between the emitter and the receiver is changed by adjusting the distance which separate them from a third body using a piezoelectric actuator. Reproduced with permission from [52]. (c) Heat flux exchanged in near-field regime between two twisted gratings. Reproduced with permission from [53]. (d) Giant thermal magnetoresistance in plasmonic structures: the thermal magnetoresistance of magneto-optical nanoparticle chains changes drastically with respect to the strength of an external magnetic field B orthogonal to the chain. Reproduced with permission from [19]. (e) Anistropic magnetoresistance: the thermal conductance between two magneto-optical particles changes with respect to the orientation of an applied magnetic field. Reproduced with permission from [58].

Optics EXPRESS

of hyperbolic bands can increase the near-field radiative heat flux in such systems [60–62] and on the other hand the application of a magnetic field enables a significant active modulation of the heat flux. However, it seems that the effective medium calculations in [57] predict an increasement of the near-field heat flux for extremely large magnetic fields, whereas the exact calculations in [59] predict a heat flux reduction for moderately large magnetic fields.

An alternative to such magneto-optical control is the electrical actuation of optical properties of materials. Among all materials, graphene-based materials [63,64], have shown to be good candidates to ensure this control. By changing the Fermi level of a graphene sheet deposited on a solid using an external gating, the scattering properties of this solid can be actively modulated [51,65–78]. This electrical actuation of optical properties of graphene-based materials has been exploited to efficiently tune and even amplify the near-field heat exchanges between two solids (see Fig. 4). The ferroelectrics state of some materials can also be tuned to control the radiative heat exchanges [79]. The active change of their spontaneous polarization can be used to shift the resonance frequency of surface phonon-polariton which some of these materials support and consequently control radiative heat transfer via varying external electric fields. Recently, three-body systems made with graphene-based materials coupled with ferroelectrics have demonstrated their strong potential to modulate near-field heat flux at kHz frequencies [80]. Finally switching and modulation of heat flux has been highlighted using metal–oxide–semiconductors (MOS). Analogously to the MOS capacitor in electronics, the accumulation and depletion of charge carriers in an ultrathin plasmonic film can be used to control the coupling of surface waves [81].

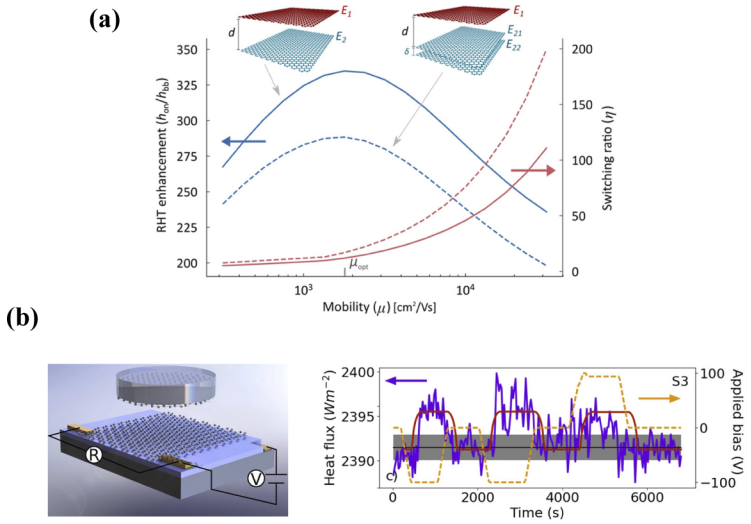

Fig. 4. (a) Radiative heat transfer enhancement (normalized to the blackbody heat transfer coefficient) and heat flux switching between two graphene sheets or between a single sheet and a stack of graphene as a function of the carrier mobility. Reproduced with permission from [74]. (b) Measured heat flux and applied bias as function time between a graphene-coated silica optical flat and a backgated, graphene-coated silicon wafer with a gate dielectric of SiO_2 and Al_2O_3 (285 nm and 8 nm, respectively). Due to a non-negligible thermal capacitance, a time delay (about 3 min) from when the bias is applied and when the heat flux change is observed can be observed. Reproduced with permission from [75].

5. Heat splitting and focusing

The directional control of radiative heat flux exchanged in near-field regime in a set of solids can be achieved using various of the before mentioned mechanisms in order to break the symmetry.

Optics EXPRESS

Hence, a heat flux splitting can be realized inside a set of pellets covered by graphene flakes by electrically tuning the Fermi level of graphene as sketched in Fig. 5(a) [82]. Such a control allows us to promote certain near-field interactions by tuning the graphene plasmons supported by the flakes.

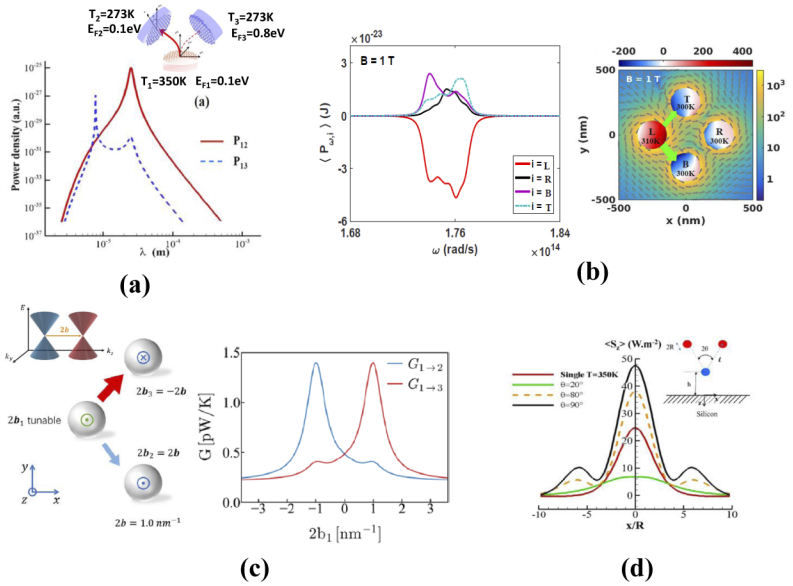

Fig. 5. (a) Graphene-based heat flux splitter. The thermal powers P_{12} and P_{13} exchanged in near-field regime between three identical pellets arranged in a symmetrical geometric configuration can be controlled by tuning the Fermi levels of graphene flakes deposited on their surface. Reproduced with permission from [82]. (b) Spectral power and heat flux lines by radiative Hall effect in a four terminal junction made of MO particles forming a square. The junction is exposed to an external magnetic field B in the direction orthogonal to the particle plane while $T_L = 310\ K$ and $T_R = T_T = T_B = 300\ K$. The mapping shows the Poynting vector field around the particles and illustrates the symmetry breaking induced by the magnetic field. Reproduced with permission from [83]. (c) Radiative thermal router consisting of three spheres of the same radius made of magnetic Weyl semimetals forming an isosceles triangle in the $x - y$ plane. By tuning the Weyl node separation $2b_1$ of the first sphere located at the apex of this triangle the thermal conductances $G_{1\to2}$ and $G_{1\to3}$ can be controlled in an asymmetric way. Reproduced with permission from [85]. (d) Heat flux focusing with a multi-tip SThM platform with three tips. The tip temperatures and their location are individually controlled, so that the thermal energy they radiate can be focused and even amplified in spots that are much smaller than those obtained with a single thermal source. Reproduced with permission from [87].

The direction of heat flux can also be modified in magneto-optical systems using an external magnetic field. Indeed, as illustrated in Fig. 5(b) [83] in four terminal junction forming a square with $C4$ symmetry, when a temperature difference $\Delta T = T_L - T_R$ is applied between the particles L and R a radiative thermal Hall effect [84] transfers heat transversally to the primary gradient bending so the overall flux. This effect results from the fact that the transmission coefficients $\mathcal{T}_{ij}$ and $\mathcal{T}_{ji}$ are not equal in nonreciprocal systems.

Thermal routers [85] based on magnetic Weyl semimetals have been recently introduced using the unique properties of optical gyrotropy. In these systems (Fig. 5(c)), which consists of three spheres made of magnetic Weyl semimetals, the heat flux direction can be controlled by moving

Optics EXPRESS

the Weyl nodes in the material using an external (magnetic or electric) field. It has also been shown that an anomalous photon thermal Hall effect can be realized in Weyl semimetals [86].

Recently, the concept of multitip scanning thermal microscopy (SThM) has been proposed [87] to locally focus and amplify the heat flux in regions much smaller than the diffraction limit and even smaller than the spot heated by a single tip. As illustrated in Fig. 5(d), the full width at half maximum (FWHM) of the spatial distribution of heat flux on the surface of substrate can be significantly reduced in comparison with that with a single tip. For specific geometric configurations, the heat flux can even locally back propagate towards the emitting system which acts in this case as a heat pump.

6. Active insulation, cooling and refrigeration

While numerous research works have been devoted to the development of nanophotonic structures to control the far-field heat exchange and enable new applications in the field of radiative cooling, little attention has been paid so far to radiative cooling at subwavelength scales. During the last years some progress have been made in this direction and new mechanisms have been proposed to actively cool down solids through near-field heat exhange. The first advance in the development of solid-state photonic cooling operating in near field has been performed in 2015 [88]. The basic idea for this cooling mechanism consists in the use of a photodiode as illustrated in Fig. 6(a) which is brought close to the solid to be cooled down. By applying an external bias voltage on the photodiode, photons are emitted with a non-vanishing chemical potential which follows from a spectral shift in the Bose-Einstein distribution function. Consequently, the apparent temperature of the photodiode can be artificially made smaller than its real temperature, so that heat can flow in the opposite direction of temperature gradient (Fig. 6(b)). Work is being performed on the photodiode, so there is no violation of any fundamental law. Moreover, the magnitude of heat exchange in the near field leads to a thermodynamic efficiency for such solid-state cooling device which is close to the Carnot limit. A proof-of-principle of this cooling principle has been demonstrated recently [89].

The active modulation of physical properties or intensive quantities has also been proposed to cool down solids through near-field interactions in two and many-body systems. Latella et al. [90] have considered radiative thermal exchange between two bodies, where the temperature of at least one body is adiabatically (slowly) modulated through interactions with external thermostats. Due to the nonlinear dependence of the temperature in the radiative heat exchange, the time average heat flux can proceed against the average temperature bias, even though instantaneously heat flows always from the hotter to the colder body. When the modulation is performed in such a way that the number of modes which participate to the transfer decreases with the temperature, a radiative shuttling effect [91] can dynamically pump heat from a body with stationary temperature in spite of a vanishing average thermal bias (Fig. 6(c)). This situation can occur, for instance, in systems made with phase-change materials whose optical properties drastically change across the phase transition. Similar heat-pumping mechanisms driven by combined modulations of positions and temperatures have been recently highlighted [92] in many-body systems.

Photonic refrigeration can also be observed in systems whose refractive index undergo a temporal modulation [93]. In these systems (Fig. 6(d)), two resonant modes such as cavities modes inside the solid to be cooled down are coupled and driven by a time modulation of refractive index. When this modulation is turned on, a fraction of the thermally generated photons from the mode of lowest energy are up-converted to the second mode and emitted in the surrounding environment. These photons carry a power (Fig. 6(e)) away from the solid with a high coefficient of performance (Fig. 6(f)).

Optics EXPRESS

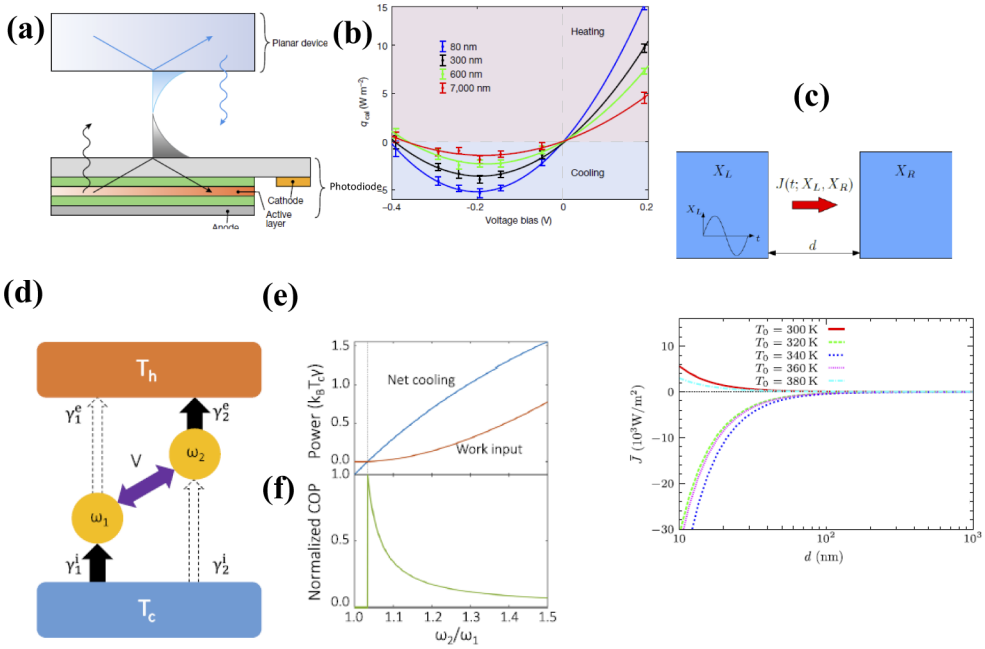

Fig. 6. (a) Photonic refrigerator working in near-field regime. By applying a bias voltage on a photodiode its apparent temperature can be reduced, so heat can be extracted from a hot solid by radiation. (b) Heat flux exchanged in the photonic refrigerator with respect with the bias voltage. Reproduced with permission from [89]. (c) Cooling by radiative heat shutting. By adiabatically modulating the temperature or the chemical potential of a solid, an extra flux superimposes to the steady state flux. Here we show the time-averaged flux $\bar{J}$ between a VO_2 slab and a sample of SiO_2 when the temperature of the VO_2 slab is $T_L(t) = T_0 + \delta T \sin(\Omega t)$ with an amplitude $\delta T = 30$ K, whereas the temperature of the other body is fixed at $T_R = T_0$. For a temperature modulation around the critical temperature of VO_2, the average flux can extract heat from the body with stationary temperature. Reproduced with permission from [90]. (d) Thermal photonic refrigerator operating between a cold solid at T_c and a hot solid at T_h. Two modes at frequencies ω_1 and ω_2 are coupled through a time-modulation of the refractive index at a time scale faster than the thermal relaxation process. (e) Net cooling power and work input as a function of the ratio of the frequencies of the two modes, for $T_h = 300$ K and $T_c = 290$ K. (f) Coefficient of performance (COP) of the refrigerator normalized to the Carnot limit. Reproduced with permission from [93].

Optics EXPRESS

7. Logical circuits

Besides the control of heat fluxes, thermal information processing at the nanoscale remains today a challenging problem. Some building blocks have been introduced during the past years in this regard, with the aim of establishing thermal analogs of conventional electronic building blocks which are driven by thermal photons rather than by electrons. Among these devices, multistable systems have been proposed to store the radiative energy [94] and to release it into the environment upon request. For example, systems composed of phase-change materials have several equilibrium (stationary) temperatures and behave like thermal memories. As shown in (Fig. 7(a)) in the particular case of a bistable system [95] which consists in two slabs of temperature T_1 and T_2, which mutually interact and which are coupled to two thermal reservoirs, two stable equilibrium temperature can exist. These states "0" and "1" correspond to the temperature pair (T_1, T_2) for which the heat flux received by each slab vanishes (Fig. 7(b)). Such states can be maintained for arbitrarily long times (Fig. 7(c)), provided that the temperatures of reservoirs are kept constant and no external perturbation modifies the net flux on each slab. By heating or cooling the slab made with the phase-change material, the thermal state of the system switch from one state to the other. This switching has been used to design self-induced thermal oscillators [96] by exploiting the hysteretic behavior of the phase-change material around its critical temperature (Figs. 7(d), 7(e)).

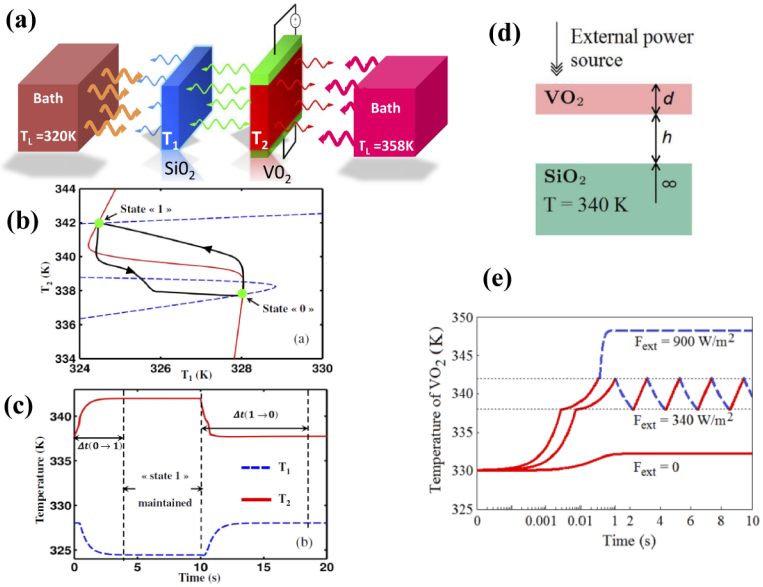

Fig. 7. (a) Sketch of a (bistable) radiative thermal memory. A membrane made of a phase transition material (VO_2) is placed at subwavelength distance from a dielectric layer (SiO_2). The system is surrounded by two thermal baths at different temperatures T_L and T_R. The temperature of the VO_2 membrane can be increased or reduced either by Joule heating or by using Peltier elements. (b) Evolution of temperatures (black line) between the two stable equilibrium temperatures (i.e. states "0" and "1"). The dashed blue and solid red lines represent the local equilibrium conditions (vanishing flux) for each membrane. (c) Time evolution of SiO_2 and VO_2 membrane temperatures. The thermal states "0" and "1" can be maintained for an arbitrarily long time, provided no external heat flux perturbs the system. Reproduced with permission from [94]. (d) Self-thermal oscillator made with a VO_2 membrane in the vicinity of a SiO_2 substrate in presence of an external constant power source F_{ext}. (e) Time evolution of the VO_2 membrane temperature at different external powers. Reproduced with permission from [96].

Optics EXPRESS

Another building block is the transistor. In electronics this device is a key element which allows for switching but above all for amplifying an electric current flowing through a solid using a simple external bias voltage. This building block is at the origin of modern electronics which have revolutionized our current life. In 2014, a radiative thermal analog of a transistor has been introduced [97]. As its electronic counterpart, the radiative transistor is a three-terminal system (Fig. 8(a)) composed by a hot body (the source), a cold body (the drain) and an intermediate slab made of a phase-change material (the gate). By operating at temperatures close to the critical temperature where the phase transition takes place in these materials, the heat flux received by the drain can be switched (Fig. 8(b)), modulated and even amplified (Fig. 8(c)) with a weak variation of the gate temperature. This behavior is closely related to the strong change in the optical properties of the phase-change material around its critical temperature. In this temperature range, the thermal resistance $R = (\frac{\partial \varphi_D}{\partial T_G})^{-1}$ defined as the variation of flux φ_D received by the drain with respect to the gate temperature T_G is negative [98]. Under these conditions, the amplification factor of the transistor $A = \mid \frac{\partial \varphi_D}{\partial \varphi_G} \mid$ can be higher than unity [46,97].

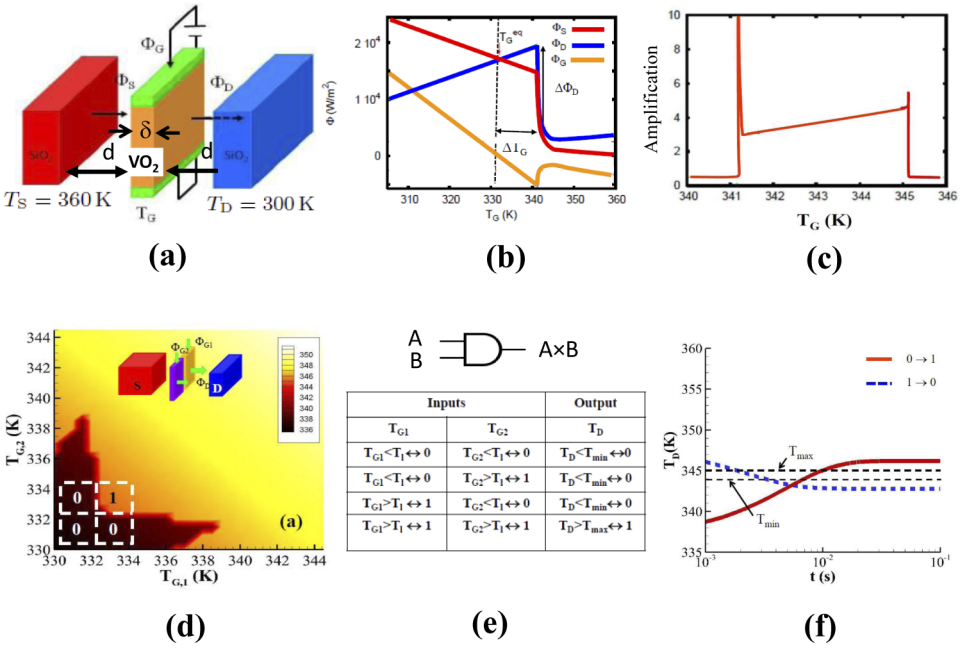

Fig. 8. (a) Radiative thermal transistor made of a three-terminal system composed of a SiO_2 source, a VO_2 gate and a SiO_2 drain. The temperature of the VO_2 gate can be actively controlled around its critical temperature by an external thermostat. (b) Radiative fluxes Φ_S, Φ_D, and Φ_G exchanged between the different parts inside the transistor when the source and the drain temperatures are fixed at $T_S = 360\,\mathrm{K}$ and $T_D = 300$ K, respectively. (c) Amplification factor with respect to the gate temperature. Reproduced with permission from [97]. (d) Radiative AND gate realized by a double SiO_2 gate thermal transistor, the source being made of SiO_2 and the drain of VO_2. The source (S) is thick (no size effect), while both gates (G1, G2) and the drain (D) have a thickness of 250 and 500 nm, respectively. The separation distances are $d = 100$ nm and the gates are assumed to be isolated one from the other. The color map represents the output T_D with respect to the two input temperatures T_{G1} and T_{G2}, the temperatures of two gates. The operating range of the AND gate is delimited by a dashed rectangular domain centered at $(T_{G1}, T_{G2}) = (T_l, T_l)$ with $T_l = 332.2$ K. (e) Truth table for the ideal AND gate. (f) Typical relaxation dynamics in a logic gate. Reproduced with permission from [99].

Optics EXPRESS

By using single or combining several radiative transistors, logic gates have been designed [99,100] to perform a Boolean treatment of information with heat exchanged in near-field regime. In Fig. 8(d) we show an example of an AND-like gate made with a double gate transistor, where the gates are made of silica and the drain is made of a phase-change material (VO_2). In this system, the temperatures T_{G1} and T_{G2} of the gates set the two inputs of the logic gate, and the temperature T_D of the drain stands for the logic gate output. By introducing a threshold value for T_D beyond which the output state of the gate switches from state "0" to state "1", we see that the system behaves as a digital AND gate (Figs. 8(d), 8(e)). The overall operating time of the logic gate corresponds to the time required to switch from one state to the other. This time is directly related to the thermalization of each element through radiative interactions, and in nanostructured systems it is of the order of few milliseconds (Fig. 8(f)).

8. Outlook

The spatio-temporal control of near-field radiative heat exchanges in complex solid architectures has opened the way to a new generation of devices for both a passive and active thermal management at nanoscale. The new degree of freedom enables the development of wireless sensors working with heat as primary source of energy rather than with electricity. In such devices, heat coming from various heat sources (machines, electric devices. . .) can be captured, stored in thermal blocks (thermal capacitors or thermal memory) and used to launch sequences of logical operations in order to either control the heat flux propagation (direction, magnitude), trigger specific actions (opto-thermo-mechanical coupling with MEMS/NEMS, ignitiate chemical reactions. . .) or even make information treatment with heat. In this perspective the operating speed of this technology could be a limiting factor. Indeed, in circuits involving interacting nanostructures the typical timescale to process one single operation is of the order of milliseconds or even more due to the thermal inertia of building blocks. For information processing this speed is obviously not competitive with the current electronic devices but it is more than enough for active thermal management and thermal sensing. For example, existing near-field probes like those developed in the last decades [101–105] can be further advanced to measure some of the theoretically proposed modulation effects locally, whereas new multi-tip or many-body setups like that in Ref. [52] are necessary to realize some of the thermotronic building blocks like the transistor. Nevertheless important progress could be done by considering 2D materials or solids far from their equilibrium where the heat carriers have different temperatures. In this last case the operating speed of thermal circuits could be reduced to few microsecond or even picoseconds, the typical relaxation time of electrons in solids. But this ultrafast physics of heat exchanges remains today a challenging problem both on a fundamental and practical point of view.

Funding. H2020 Marie Skłodowska-Curie Actions (892718); Deutsche Forschungsgemeinschaft, Heisenberg Programme (404073166); Agence Nationale de la Recherche (ANR-Computheat-MRSEI-6786).

Disclosures. The authors declare no conflicts of interest.

Data availability. No data were generated or analyzed in the presented research.

References

1. F. Braun, "Uber die Stromleitung durch Schwefelmetalic," Annalen der Physik und Chemie **153**, 556 (1874).
2. J. Bardeen and W. H. Brattain, "The Transistor, A Semi-Conductor Triode," Phys. Rev. **74**(2), 230–231 (1948).
3. B. Li, L. Wang, and G. Casati, "Thermal Diode: Rectification of Heat Flux," Phys. Rev. Lett. **93**(18), 184301 (2004).
4. B. Li and L. Wang and G. Casati, "Negative differential thermal resistance and thermal transistor," Appl. Phys. Lett. **88**(14), 143501 (2006).
5. C. W. Chang, D. Okawa, A. Majumdar, and A. Zettl, "Solid-State Thermal Rectifier," Science **314**(5802), 1121–1124 (2006).
6. N. Li, J. Ren, L. Wang G. Zhang, P. Hanggi, and B. Li, "Phononics: Manipulating heat flow with electronic analogs and beyond," Rev. Mod. Phys. **84**(3), 1045–1066 (2012).
7. Y. Li, W. Li, T. Han, X. Zheng, J. Li, B. Li, S. Fan, and C.-W. Qiu, "Transforming heat transfer with thermal metamaterials and devices," Nat. Rev. Mater. **6**(6), 488–507 (2021).

Optics EXPRESS

8. M. Planck, *The Theory of Heat Radiation* (Blakiston's Son & Co, 1914).
9. E. Cravalho, C. Tien, and R. Caren, "Effect of small spacings on radiative transfer between two dielectrics," J. Heat Transfer **89**(4), 351–358 (1967).
10. D. Polder and M. Van Hove, "Theory of Radiative Heat Transfer between Closely Spaced Bodies," Phys. Rev. B **4**(10), 3303–3314 (1971).
11. J. B. Pendry, "Radiative exchange of heat between nanostructures," J. Phys.: Condens. Matter **11**(35), 6621–6633 (1999).
12. K. Joulain, J.-P. Mulet, F. Marquier, R. Carminati, and J.-J. Greffet, "Surface electromagnetic waves thermally excited: Radiative heat transfer, coherence properties and Casimir forces revisited in the near field," Surf. Sci. Rep. **57**(3-4), 59–112 (2005).
13. A. I. Volokitin and B. N. J. Persson, "Near-field radiative heat transfer and noncontact friction," Rev. Mod. Phys. **79**(4), 1291–1329 (2007).
14. S. M. Rytov, Y. A. Kravtsov, and V. I. Tatarskii, *Principles of Statistical Radiophysics*, Vol. 3 (Springer, New York, 1989).
15. W. Eckhardt, "Macroscopic theory of electromagnetic fluctuations and stationary radiative heat transfer," Phys. Rev. A **29**(4), 1991–2003 (1984).
16. P. Ben-Abdallah, S.-A Biehs, and K. Joulain, "Many-body radiative heat transfer theory," Phys. Rev. Lett. **107**(11), 114301 (2011).
17. I. Latella, P. Ben-Abdallah, S.-A. Biehs, M. Antezza, and R. Messina, "Radiative heat transfer and nonequilibrium Casimir-Lifshitz force in many-body systems with planar geometry," Phys. Rev. B **95**(20), 205404 (2017).
18. M. Krüger, G. Bimonte, T. Emig, and M. Kardar, "Trace formulas for nonequilibrium Casimir interactions, heat radiation, and heat transfer for arbitrary objects," Phys. Rev. B **86**(11), 115423 (2012).
19. I. Latella and P. Ben-Abdallah, "Giant Thermal Magnetoresistance in Plasmonic Structures," Phys. Rev. Lett. **118**(17), 173902 (2017).
20. S.-A. Biehs, R. Messina, P. S. Venkataram, A. W. Rodriguez, J. C. Cuevas, and P. Ben-Abdallah, "Near-field Radiative Heat Transfer in Many-Body Systems," arXiv:2007.05604 [cond-mat.mes-hall], https://arxiv.org/abs/2007.05604.
21. C. R. Otey, W. T. Lau, and S. Fan, "Thermal Rectification through Vacuum," Phys. Rev. Lett. **104**(15), 154301 (2010).
22. H. Iizuka and S. Fan, "Rectification of evanescent heat transfer between dielectric-coated and uncoated silicon carbide plates," J. Appl. Phys. **112**(2), 024304 (2012).
23. S. Basu and M. Francoeur, "Near-field radiative transfer based thermal rectification using doped silicon," Appl. Phys. Lett. **98**(11), 113106 (2011).
24. L. P. Wang and Z. M. Zhang, "Thermal Rectification Enabled by Near-Field Radiative Heat Transfer Between Intrinsic Silicon and a Dissimilar Material," Nanoscale Microscale Thermophys. Eng. **17**(4), 337–348 (2013).
25. L. Zhu, C. R. Otey, and S. Fan, "Ultrahigh-contrast and large-bandwidth thermal rectification in near-field electromagnetic thermal transfer between nanoparticles," Phys. Rev. B **88**(18), 184301 (2013).
26. G. Xu, J. Sun, H. Mao, and T. Pan, "Surface plasmon-enhanced near-field thermal rectification in graphene-based structures," J. Appl. Phys. **124**(18), 183104 (2018).
27. P. Ben-Abdallah and S.-A. Biehs, "Phase-change radiative thermal diode," Appl. Phys. Lett. **103**(19), 191907 (2013).
28. Y. Yang, S. Basu, and L. Wang, "Radiation-based near-field thermal rectification with phase transition materials," Appl. Phys. Lett. **103**(16), 163101 (2013).
29. J. G. Huang, Q. Li, Z. H. Zheng, and Y. M. Xuan, "Thermal rectification based on thermochromic materials," Int. J. Heat Mass Transfer **67**, 575–580 (2013).
30. W. Gu, G.-H. Tang, and W.-Q. Tao, "Thermal switch and thermal rectification enabled by near-field radiative heat transfer between three slabs," Int. J. Heat Mass Transfer **82**, 429–434 (2015).
31. A. Ghanekar, J. Ji, and Y. Zheng, "High-rectification near-field thermal diode using phase change periodic nanostructure," Appl. Phys. Lett. **109**(12), 123106 (2016).
32. Z. H. Zheng, X. L. Liu, A. Wang, and Y. M. Xuan, "Graphene-assisted near-field radiative thermal rectifier based on phase transition of vanadium dioxide (VO_2)," Int. J. Heat Mass Transfer **109**(12), 63–72 (2017).
33. A. Ghanekar, Y. Tian, M. Ricci, S. Zhang, O. Gregory, and Y. Zheng, "Near-field thermal rectification devices using phase change periodic nanostructure," Opt. Express **26**(2), A209 (2018).
34. F. Chen, X. Liu, Y. Tian, and Y. Zheng, "Dynamic Tuning of Near-Field Radiative Thermal Rectification," Adv. Eng. Mater. **23**, 2000825 (2021).
35. A. S. Barker, H. W. Verleur, and H. J. Guggenheim, "Infrared optical properties of vanadium dioxide above and below the transition temperature," Phys. Rev. Lett. **17**(26), 1286–1289 (1966).
36. M. M. Qazilbash, M. Brehm, B.-G. BChae, P.-C. Ho, G. O. Andreev, B.-J. BKim, S. J. BYun, A. V. Balatsky, M. B. Maple, F. Keilmann, H.-T. BKim, and D. N. Basov, "Mott transition in VO_2 revealed by infrared spectroscopy and nano-imaging," Science **318**(5857), 1750–1753 (2007).
37. K. Ito, K. Nishikawa, H. Lizuka, and H. Toshiyoshi, "Experimental investigation of radiative thermal rectifier using vanadium dioxide," Appl. Phys. Lett. **105**(25), 253503 (2014).
38. I. Y. Forero-Sandoval, J. A. Chan-Espinoza, J. Ordonez-Miranda, J. J. Alvarado-Gil, F. Dumas-Bouchiat, C. Champeaux, K. Joulain, Y. Ezzahri, J. Drevillon, C. L. Gomez-Heredia, and J. A. Ramirez-Rincon, "VO_2 Substrate Effect on the Thermal Rectification of a Far-Field Radiative Diode," Phys. Rev. Appl. **14**(3), 034023 (2020).

Optics EXPRESS

39. A. Fiorino, Anthony, D. Thompson, L. Zhu, R. Mittapally, S.-A. Biehs, O. Bezencenet, N. El-Bondry, S. Bansropun, P. Ben-Abdallah, E. Meyhofer, and P. Reddy, "A Thermal Diode Based on Nanoscale Thermal Radiation," ACS Nano **12**(6), 5774–5779 (2018).
40. P. J. van Zwol, K. Joulain, P. Ben-Abdallah, J.-J. Greffet, and J. Chevrier, "Fast nanoscale heat-flux modulation with phase-change materials," Phys. Rev. B **83**(20), 201404 (2011).
41. P. van Zwol, K. Joulain, P. Ben-Abdallah, and J. Chevrier, "Phonon polaritons enhance near-field thermal transfer across the phase transition of VO_2," Phys. Rev. B **84**(16), 161413 (2011).
42. T. Kralik, V. Musilova, T. Fort, and A. Srnka, "Effect of superconductivity on near-field radiative heat transfer," Phys. Rev. B **95**(6), 060503 (2017).
43. V. Musilova, T. Kralik, T. Fort, and M. Macek, "Strong suppression of near-field radiative heat transfer by superconductivity in NbN," Phys. Rev. B **99**(2), 024511 (2019).
44. E. Nefzaoui, K. Joulain, J. Drevillon, and Y. Ezzahri, "Radiative thermal rectification using superconducting materials," Appl. Phys. Lett. **104**(10), 103905 (2014).
45. J. Ordonez-Miranda, K. Joulain, D. De Sousa Meneses, Y. Ezzahri, and J. Drevillon, "Photonic thermal diode based on superconductors," J. Appl. Phys. **122**(9), 093105 (2017).
46. E. Moncada-Villa and J. C. Cuevas, "Normal-Metal-Superconductor Near-Field Thermal Diodes and Transistors," Phys. Rev. Appl. **15**(2), 024036 (2021).
47. A. Ott, R. Messina, P. Ben-Abdallah, and S.-A. Biehs, "Radiative thermal diode driven by nonreciprocal surface waves," Appl. Phys. Lett. **114**(16), 163105 (2019).
48. I. Latella, P. Ben-Abdallah, and M. Nikbakht, "Radiative thermal rectification in many-body systems," Phs. Rev. B **104**, 045410 (2021).
49. R. St. Gelais, L. Zhu, S. Fan, and M. Lipson, "Near-field radiative heat transfer between parallel structures in the deep subwavelength regime," Nat. Nanotechnol. **11**(6), 515–519 (2016).
50. G. R. Bhatt, B. Zhao, S. Roberts, I. Datta, A. Mohanty, T. Lin, J.-M. Hartmann, R. St-Gelais, S. Fan, and M. Lipson, "Integrated near-field thermo-photovoltaics for heat recycling," Nat. Commun. **11**(1), 2545 (2020).
51. M. Lim, S. S. Lee, and B. Jae Lee, "Near-field thermal radiation between graphene-covered doped silicon plates," Opt. Express **21**(19), 22173 (2013).
52. D. Thompson, L. Zhu, E. Meyhofer, and P. Reddy, "Nanoscale radiative thermal switching via multi-body effects," Nat. Nanotechnol. **15**(2), 99–104 (2020).
53. S.-A. Biehs, F. S. S. Rosa, and P. Ben-Abdallah, "Modulation of near-field heat transfer between two gratings," Appl. Phys. Lett. **98**(24), 243102 (2011).
54. X. Wu and C. Fu, "Near-field radiative modulator based on dissimilar hyperbolic materials with in-plane anisotropy," Int. J. Heat Mass Transfer **168**, 120908 (2021).
55. G. T. Papadakis, C. J. Ciccarino, L. Fan, M. Orenstein, P. Narang, and S. Fan, "Deep-Subwavelength Thermal Switch via Resonant Coupling in Monolayer Hexagonal Boron Nitride," Phys. Rev. Appl. **15**(5), 054002 (2021).
56. E. Moncada-Villa, V. Fernández-Hurtado, F. J. García-Vidal, A. García-Martín, and J. C. Cuevas, "Magnetic-field control of near-field radiative heat transfer and the realization of highly tunable hyperbolic thermal emitters," Phys. Rev. B **92**(12), 125418 (2015).
57. E. Moncada-Villa and J. C. Cuevas, "Magnetic field effects in the near-field radiative heat transfer between planar structures," Phys. Rev. B **101**(8), 085411 (2020).
58. R. M. Abraham Ekeroth, P. Ben-Abdallah, J. C. Cuevas, and A. García-Martín, "Anisotropic Thermal Magnetoresistance for an Active Control of Radiative Heat Transfer," ACS Photonics **5**(3), 705–710 (2018).
59. E. Moncada-Villa and J. C. Cuevas, "Near-field radiative heat transfer between one-dimensional magnetophotonic crystals," Phys. Rev. B **103**(7), 075432 (2021).
60. S. A. Biehs, M. Tschikin, and P. Ben-Abdallah, "Hyperbolic metamaterials as an analog of a blackbody in the near field," Phys. Rev. Lett. **109**(10), 104301 (2012).
61. Y. Guo, C. L. Cortes, S. Molesky, and Z. Jacob, "Broadband super-Planckian thermal emission from hyperbolic metamaterials," Appl. Phys. Lett. **101**(13), 131106 (2012).
62. H. Iizuka and S. Fan, "Significant Enhancement of Near-Field Electromagnetic Heat Transfer in a Multilayer Structure through Multiple Surface-States Coupling," Phys. Rev. Lett. **120**(6), 063901 (2018).
63. K. S. Novoselov, A. K. Geim, S. V. Morozov, D. Jiang, Y. Zhang, S. V. Dubonos, I. V. Grigorieva, and A. A. Firsov, "Electric field effect in atomically thin carbon films," Science **306**(5696), 666–669 (2004).
64. A. K. Geim and K. S. Novoselov, "The rise of graphene," Nat. Mater. **6**(3), 183–191 (2007).
65. A. I. Volokitin and B. N. J. Persson, "Near-field radiative heat transfer between closely spaced graphene and amorphous SiO_2," Phys. Rev. B **83**(24), 241407 (2011).
66. V. B. Svetovoy, P. J. van Zwol, and J. Chevrier, "Plasmon enhanced near-field radiative heat transfer for graphene covered dielectrics," Phys. Rev. B **85**(15), 155418 (2012).
67. O. Ilic, M. Jablan, J. D. Joannopoulos, I. Celanovic, H. Buljan, and M. Soljacic, "Near-field thermal radiation transfer controlled by plasmons in graphene," Phys. Rev. B **85**(15), 155422 (2012).
68. P. Rodriguez-Lopez, W.-K. Tse, and D. A. R. Dalvit, "Radiative heat transfer in 2D Dirac materials," J. Phys.: Condens. Matter **27**(21), 214019 (2015).
69. P. J. van Zwol, S. Thiele, C. Berger, W. A. de Heer, and J. Chevrier, "Nanoscale Radiative Heat Flow due to Surface Plasmons in Graphene and Doped Silicon," Phys. Rev. Lett. **109**(26), 264301 (2012).

Optics EXPRESS

70. J. Yang, W. Du, Y. Su, Y. Fu, S. Gong, S. He, and Y. Ma, "Observing of the super-Planckian near-field thermal radiation between graphene sheets," Nat. Commun. **9**(1), 4033 (2018).
71. O. Ilic, M. Jablan, J. D. Joannopoulos, I. Celanovic, and M. Soljacic, "Overcoming the black body limit in plasmonic and graphene near-field thermophotovoltaic systems," Opt. Express **20**(S3), A366 (2012).
72. R. Messina and P. Ben-Abdallah, "Graphene-based photovoltaic cells for near-field thermal energy conversion," Sci. Rep. **3**(1), 1383 (2013).
73. Y. Yang and L. Wang, "Electrically-controlled near-field radiative thermal modulator made of graphene-coated silicon carbide plates," J. Quant. Spectrosc. Radiat. Transfer **197**, 68–75 (2017).
74. O. Ilic, N. H. Thomas, T. Christensen, M. C. Sherrott, M. Soljacic, A. J. Minnich, O. D. Miller, and H. A. Atwater, "Active Radiative Thermal Switching with Graphene Plasmon Resonators," ACS Nano **12**(3), 2474–2481 (2018).
75. N. H. Thomas, M. C. Sherrott, J. Broulliet, H. A. Atwater, and A. J. Minnich, "Electronic Modulation of Near-Field Radiative Transfer in Graphene Field Effect Heterostructures," Nano Lett. **19**(6), 3898–3904 (2019).
76. M.-J. He, H. Qi, Y.-T. Ren, Y.-J. Zhao, and M. Antezza, "Magnetoplasmonic manipulation of nanoscale thermal radiation using twisted graphene gratings," Int. J. Heat Mass Transfer **150**, 119305 (2020).
77. M. He, H. Qi, Y. Ren, Y. Zhao, and M. Antezza, "Active control of near-field radiative heat transfer by a graphene-gratings coating-twisting method," Opt. Lett. **45**(10), 2914–2917 (2020).
78. R. Messina, P. Ben-Abdallah, B. Guizal, and M. Antezza, "Graphene-based amplification and tuning of near-field radiative heat transfer between dissimilar polar materials," Phys. Rev. B **96**(4), 045402 (2017).
79. Y. Huang, S. V. Boriskina, and G. Chen, "Electrically tunable near-field radiative heat transfer via ferroelectric materials," Appl. Phys. Lett. **105**(24), 244102 (2014).
80. I. Latella and P. Ben-Abdallah, "Graphene-based autonomous pyroelectric system for near-field energy conversion,", arXiv:2104.05564 [cond-mat.mes-hall], https://arxiv.org/abs/2104.05564.
81. G. T. Papadakis, B. Zhao, S. Buddhiraju, and S. Fan, "Gate-Tunable Near-Field Heat Transfer," ACS Photonics **6**(3), 709–719 (2019).
82. P. Ben-Abdallah, A. Belarouci, L. Frechette, and S.-A. Biehs, "Heat flux splitter for near-field thermal radiation," Appl. Phys. Lett. **107**(5), 053109 (2015).
83. A. Ott, R. Messina, P. Ben-Abdallah, and S.-A. Biehs, "Magnetothermoplasmonics: from theory to applications," J. Photon. Energy **9**(3), 032711 (2019).
84. P. Ben-Abdallah, "Photon thermal Hall effect," Phys. Rev. Lett. **116**(8), 084301 (2016).
85. C. Guo, B. Zhao, D. Huang, and S. Fan, "Radiative Thermal Router Based on Tunable Magnetic Weyl Semimetals," ACS Photonics **7**(11), 3257–3263 (2020).
86. A. Ott, S.-A. Biehs, and P. Ben-Abdallah, "Anomalous photon thermal Hall effect," Phys. Rev. B **101**(24), 241411 (2020).
87. P. Ben-Abdallah, "Multitip Near-Field Scanning Thermal Microscopy," Phys. Rev. Lett. **123**(26), 264301 (2019).
88. K. Chen, P. Santhanam, S. Sandhu, L. Zhu, and S. Fan, "Heat-flux control and solid-state cooling by regulating chemical potential of photons in near-field electromagnetic heat transfer," Phys. Rev. B **91**(13), 134301 (2015).
89. L. Zhu, A. Fiorino, D. Thompson, R. Mittapally, E. Meyhofer, and P. Reddy, "Near-field photonic cooling through control of the chemical potential of photons," Nature **566**(7743), 239–244 (2019).
90. I. Latella, R. Messina, J. M. Rubi, and P. Ben-Abdallah, "Radiative Heat Shuttling," Phys. Rev. Lett. **121**(2), 023903 (2018).
91. N.-B. Li, F. Zhan, P. Hanggi, and B. Li, "Shuttling heat across one-dimensional homogenous nonlinear lattices with a Brownian heat motor," Phys. Rev. E **80**(1), 011125 (2009).
92. R. Messina and P. Ben-Abdallah, "Many-body near-field radiative heat pumping," Phys. Rev. B **101**(16), 165435 (2020).
93. S. Buddhiraju, W. Li, and S. Fan, "Photonic Refrigeration from Time-Modulated Thermal Emission," Phys. Rev. Lett. **124**(7), 077402 (2020).
94. V. Kubytskyi, S.-A. Biehs, and P. Ben-Abdallah, "Radiative Bistability and Thermal Memory," Phys. Rev. Lett. **113**(7), 074301 (2014).
95. C. Khandekar and A. W. Rodriguez, "Thermal bistability through coupled photonic resonances," Appl. Phys. Lett. **111**(8), 083104 (2017).
96. S. A. Dyakov, J. Dai, M. Yan, and M. Qiu, "Thermal self-oscillations in radiative heat exchange," Appl. Phys. Lett. **106**(6), 064103 (2015).
97. P. Ben-Abdallah and S.-A. Biehs, "Near-field thermal transistor," Phys. Rev. Lett. **112**(4), 044301 (2014).
98. L. Zhu, C. R. Otey, and S. Fan, "Negative differential thermal conductance through vacuum," Appl. Phys. Lett. **100**(4), 044104 (2012).
99. P. Ben-Abdallah and S.-A. Biehs, "Towards boolean operations with thermal photons," Phys. Rev. B **94**(24), 241401 (2016).
100. C. Kathmann, M. Reina, R. Messina, P. Ben-Abdallah, and S.-A. Biehs, "Scalable radiative thermal logic gates based on nanoparticle networks," Sci. Rep. **10**(1), 3596 (2020).
101. A. Kittel, U. Wischnath, J. Welker, O. Huth, F. Rüting, and S.-A. Biehs, "Near-field thermal imaging of nanostructured surfaces," Appl. Phys. Lett. **93**(19), 193109 (2008).
102. F. Huth, M. Schnell, J. Wittborn, N. Ocelic, and R. Hillenbrand, "Materials for multifunctional balloon catheters with capabilities in cardiac electrophysiological mapping and ablation therapy," Nat. Mater. **10**(4), 316–323 (2011).

Optics EXPRESS

103. Y. De Wilde, F. Formanek, R. Carminati, B. Gralak, P.-A. Lemoine, K. Joulain, J.-P. Mulet, Y. Chen, and J.-J. Greffet, "Thermal radiation scanning tunnelling microscopy," Nature **444**(7120), 740–743 (2006).
104. A. C. Jones and M. B. Raschke, "Thermal Infrared Near-Field Spectroscopy," Nano Lett. **12**(3), 1475–1481 (2012).
105. Q. Weng, S. Komiyama, Z. An, L. Yang, P. Chen, S.-A. Biehs, Y. Kajihara, and W. Lu, "Imaging of nonlocal hot-electron energy dissipation via shot noise," Science **360**, 775 (2018).

92.178.243.95 {ts '2021-07-20 10:34:35'}